Biogeosciences, 22, 4531–4544, 2025
https://doi.org/10.5194/bg-22-4531-2025

Biogeosciences Open Access EGU

Research article

Projections of coral reef carbonate production from a global climate–coral reef coupled model

Nathaelle Bouttes[1], **Lester Kwiatkowski**[2], **Elodie Bougeot**[3], **Manon Berger**[1], **Victor Brovkin**[4,5], **and Guy Munhoven**[6]

[1]Laboratoire des Sciences du Climat et de l'Environnement, LSCE/IPSL, CEA-CNRS-UVSQ, Université Paris-Saclay, Gif-sur-Yvette, 91191, France
[2]LOCEAN Laboratory, Sorbonne Université-CNRS-IRD-MNHN, Paris, 75005, France
[3]LMD-IPSL, CNRS, Ecole Normale Supérieure/PSL Res. Univ, Ecole Polytechnique, Sorbonne Université, Paris, 75005, France
[4]Max Planck Institute for Meteorology, Hamburg, 20146, Germany
[5]CEN, University of Hamburg, Hamburg, 20146, Germany
[6]Dépt. d'Astrophysique, de Géophysique et d'Océanographie, Université de Liège, Liège, 4000, Belgium

Correspondence: Nathaelle Bouttes (nathaelle.bouttes@lsce.ipsl.fr)

Received: 29 November 2024 – Discussion started: 9 December 2024
Revised: 28 April 2025 – Accepted: 20 June 2025 – Published: 11 September 2025

Abstract. Coral reefs are under threat due to climate change and ocean acidification. However, large uncertainties remain concerning future carbon dioxide emissions, climate change and the associated impacts on coral reefs. While most previous studies have used climate model outputs to compute future coral reef carbonate production, we use a coral reef carbonate production module embedded in a global carbon–climate model. This enables the simulation of the response of coral reefs to projected changes in physical and chemical conditions at finer temporal resolution. The use of a fast-intermediate complexity model also permits the simulation of a large range of possible futures by considering different greenhouse gas concentration scenarios (Shared Socioeconomic Pathways (SSPs)) and different climate sensitivities (hence different levels of warming for a given level of acidification), as well as the possibility of corals adapting their thermal bleaching thresholds. We show that without thermal adaptation, global coral reef carbonate production decreases to less than 25 % of historical values in most scenarios over the 21st century, with limited further declines between 2100 and 2300 irrespective of the climate sensitivity. With thermal adaptation, there is far greater scenario variability in projections of reef carbonate production. Under high-emission scenarios the rate of 21st century declines is attenuated, with some global carbonate production declines delayed until the 22nd century. Under high-mitigation scenarios, however, global coral reef carbonate production can recover in the 21st and 22nd centuries and thereafter persist at 50 %–90 % of historical values, provided that the climate sensitivity is moderate.

1 Introduction

Coral reefs are marine ecosystems composed of reef-building corals. The corals build structures (exoskeletons) made of calcium carbonate in the form of aragonite. The carbonate structures not only provide a habitat for many marine species, but also play a role in the carbon cycle. Indeed, the production of calcium carbonate modifies the carbonate equilibrium in the ocean, which can ultimately modify the atmospheric CO_2 concentration and impact climate. Understanding and modeling carbonate production is therefore crucial for both quantifying reefs impacts and anticipating possible climate feedbacks.

While coral reefs are among the most diverse and valuable ecosystems on Earth, they are under multiple threats due to human-induced changes to their environment (Pandolfi et al., 2011; Hoegh-Guldberg et al., 2017). With increasing atmospheric carbon dioxide concentrations, marine organisms face ocean warming and ocean acidification. Climate models indicate that under the high-emission scenario

Published by Copernicus Publications on behalf of the European Geosciences Union.

SSP5-8.5 (Shared Socioeconomic Pathway), sea surface temperatures will increase by $3.47 \pm 0.78\,^{\circ}\mathrm{C}$, while the surface pH will decrease by -0.44 ± 0.005 by the end of the century (multi-model global mean change values of 2080–2099 relative to 1870–1899 ± the intermodel standard deviation; Kwiatkowski et al., 2020). With the low-emission scenario SSP1-2.6, sea surface temperatures (SSTs) are still projected to increase, albeit to a lesser extent, by $1.42 \pm 0.32\,^{\circ}\mathrm{C}$. The surface pH decrease is also smaller, of -0.16 ± 0.002. Not only will temperatures increase, but marine heat waves will become longer lasting and more frequent (Frölicher et al., 2018).

Both ocean warming and acidification have negative effects on coral reefs. Increased seawater temperatures, and in particular increased marine heat wave frequency and intensity, is damaging for coral reefs (Cooley et al., 2022). Under heat stress, coral polyps expel their zooxanthellae symbionts, resulting in coral bleaching (Brown, 1997; Hoegh-Guldberg, 1999; Sully et al., 2019). Depending on the rate at which seawater temperatures return to climatological levels of the early and mid-20th century, corals can recover and zooxanthellae symbiosis can resume (DeCarlo et al., 2019; Logan et al., 2021). However, under extreme or repeated heat stress, bleaching becomes severe and can lead to the coral death.

The calcification process which enables organisms to produce their external calcium carbonate skeleton requires more energy as the oceans take up anthropogenic carbon and acidify. To characterize this we consider the aragonite saturation state (Ω_{ar}) defined as the ratio of the product of calcium and carbonate ion concentrations to the equilibrium thermodynamic solubility product (K_{sp}) for the mineral aragonite at in situ temperature, salinity and pressure:

$$\Omega_{\mathrm{ar}} = \frac{[\mathrm{Ca}^{2+}][\mathrm{CO}_3^{2-}]}{K_{\mathrm{sp}}}. \quad (1)$$

With decreasing carbonate ion concentration (e.g., as a result of surface ocean acidification), the saturation state is reduced, which can lead to decreased coral reef calcification (Chan and Connolly, 2013; Albright et al., 2018). It also leads to higher dissolution, which could lead to coral reefs becoming net dissolving when atmospheric CO_2 reaches 560 ppm (Silverman et al., 2009), which is expected to occur by ∼ 2050 (Eyre et al., 2018).

Numerous studies have investigated the impact of warming and/or acidification on coral reef organisms, either in situ (e.g., Albright et al., 2016, 2018; Sully et al., 2019) or in mesocosms/laboratories (e.g., Dove et al., 2013). Based on such studies, numerical and statistical models have been developed and used to evaluate the impact of temperature and ocean acidification changes on coral reefs, often regionally (Evenhuis et al., 2015; Buddemeier et al., 2008, 2011; Sully et al., 2022) but also globally (Kleypas et al., 1999; Donner et al., 2005; Silverman et al., 2009; Frieler et al., 2012; Couce et al., 2013; van Hooidonk et al., 2014; Eyre et al., 2018; Cornwall et al., 2021). Among the models used to evaluate the impact on coral reefs during the next century globally, some considered the impact of future temperature change (Donner et al., 2005), others the impact of Ω_{ar} or pH change (Kleypas et al., 1999; Eyre et al., 2018), and some both variables simultaneously (Silverman et al., 2009; Frieler et al., 2012; Couce et al., 2013; van Hooidonk et al., 2014; Cornwall et al., 2021; Cornwall et al., 2023). These coral reef models were not embedded within climate models; hence they were forced by climate data outputs that are often only stored at monthly resolution. This means that daily temperature could not always be used, preventing accurate bleaching effect computation. In addition, the aragonite saturation state (Ω_{ar}) is also often not stored, further hindering accounting for this effect. Here we use a coupled numerical climate–carbon cycle model that includes a coral reef module (Bouttes et al., 2024), allowing us to evaluate the dynamics of coral reef carbonate production as a function of temperature and Ω_{ar} on daily timescales. The use of this coupled model allows us to evaluate the individual and combined impact of ocean warming and acidification to test possible nonlinearities.

In addition, future coral carbonate production is difficult to project due to several sources of uncertainties. (i) Different emission scenarios will yield different evolution pathways of climate and ocean acidification (Kwiatkowski et al., 2020). Past studies have tested the impact of different scenarios (Cornwall et al., 2021, 2023), but they were restrained to the old Representative Concentration Pathway (RCP) scenarios. Here we span the different SSP scenarios (Meinshausen et al., 2020) that are currently used as inputs for state-of-the-art global climate models. (ii) Different climate models that have various climate sensitivities (Forster et al., 2020; Meehl et al., 2020; Forster et al., 2021) result in different climate and ocean acidification evolutions for the same emission scenario. To account for this uncertainty, we use different versions of the iLOVECLIM climate model (see Sect. 2.1.1) spanning the range of climate sensitivities in climate models. (iii) Potential coral adaptation to thermal bleaching could also result in different coral reef carbonate production (Cornwall et al., 2023). Hence, we use two versions of the coral reef model: with and without adaptation. We make use of the fast coral–carbon–climate model to evaluate the impact of all three sources of uncertainties in future projections.

2 Methods

We use iLOVECLIM, a coupled climate–carbon cycle model which includes a new module of calcium carbonate production by coral reefs called iCORAL (Bouttes et al., 2023).

2.1 The iLOVECLIM-iCORAL climate model with coral reefs

2.1.1 iLOVECLIM carbon–climate model

iLOVECLIM is an intermediate complexity model including an atmosphere (ECBILT), an ocean (CLIO), a sea ice (LIM) and a continental vegetation (VECODE) module inherited from the LOVECLIM model (Goosse et al., 2010). The ocean model has a horizontal resolution of 3° with 20 vertical levels; the atmosphere has a horizontal resolution of 5.6° with 3 levels. It is also coupled to an ocean carbon cycle module (Bouttes et al., 2015). The ocean carbon cycle module includes two types of plankton (phytoplankton and zooplankton), labile and refractory dissolved organic carbon (respectively DOC and DOCs), dissolved inorganic carbon (DIC), alkalinity (ALK), and nutrients (PO4). The total particulate production that gets exported from the euphotic zone is progressively remineralized below. Phytoplankton, zooplankton, DOC, DOCs, DIC, ALK and nutrients are all transported (by advection/diffusion) in the ocean. The iLOVECLIM model is relatively fast with around 700 simulated years per day, making it well suited for both long-duration and large-ensemble simulations.

2.1.2 iCORAL coral reef carbonate production module

A coral module has recently been added in iLOVECLIM (iCORAL; Bouttes et al., 2024). It is based on the ReefHab model (Kleypas, 1995, 1997) with some modifications and add-ons. In each grid cell of the model, the module computes habitability, i.e., the possibility of coral reef development depending on temperature, salinity, phosphate concentration and light limitation. Carbonate production can take place provided that

- the temperature is between 18.1 and 31.5 °C and exceeds 18.1 °C throughout the year
- the salinity is between 30 and 39
- the phosphate concentration is below 0.2 µmol L^{-1}
- the depth Z is shallower than the maximum coral production depth (Z_{max}), which depends on attenuation of light in the water column:

$$Z_{\max} = \frac{\log\left(\frac{I_{\min}}{\mathrm{PAR}}\right)}{K_{490}}, \tag{2}$$

where I_{min} is a fixed parameter (the minimum light intensity necessary for reef growth), PAR is the photosynthetically active radiation at the surface (computed by the iLOVECLIM climate model), and K_{490} is the diffuse attenuation coefficient at 490 nm taken from the Level-3 binned MODIS-Aqua products in the OceanColor database (available at: http://oceancolor.gsfc.nasa.gov, last access: 14 June 2014). The production depth is defined as the depth at which light is at the I_{min} level.

In habitable zones, coral reef carbonate production P is computed on a vertical subgrid with a 1 m resolution from the available PAR, temperature T, aragonite saturation state Ω_{ar}, surface area S_{avail} and a topographic factor TF, following

$$P = g_{\max} \times f_R\,(\mathrm{PAR}) \times f_T\,(T) \times f_O\,(\Omega_{\mathrm{ar}}) \times S_{\mathrm{avail}} \times \mathrm{TF} \times f_{\mathrm{B}}\,(t; t_{\mathrm{bleach}}), \tag{3}$$

where g_{max} is the maximum value (fixed) and $f_B(t; t_{bleach})$ a function for the bleaching.

The two main potential drivers of production changes in the future are temperature and saturation state, as they will evolve in the future. In the coral module, the temperature function $f_T(T)$ is a linear function of temperature (T, in °C) fitted for the temperature range of coral reef habitability ($f_T(T) = 0$ at $T = 18.1$ °C and $f_T(T) = 1$ at $T = 31.5$ °C; $f_T(T) = 0$ outside the range of 18.1–31.5 °C):

$$f\,(T) = -1.38 + 0.077 \times T. \tag{4}$$

Following Langdon and Atkinson (2005), the saturation state function $f_O(\Omega_{ar})$ is as follows:

$$\text{if } \Omega > 1 \quad f_O\,(\Omega) = \frac{\Omega - 1}{K_{\mathrm{omega}}}, \tag{5}$$

$$\text{else } f_O\,(\Omega) = 0, \tag{6}$$

with K_{omega} a normalization parameter ($K_{omega} = 2.86$).

The module assumes the possibility of having coral development as soon as the conditions are favorable, without considering larvae dispersion. In developments to ReefHab, we have added temperature and Ω_{ar} as variables used to compute coral reef carbonate production. The impact of bleaching on carbonate production is also accounted for with options for coral reef recovery times following bleaching events of differing intensity (see Bouttes et al., 2024, for details and Sect. 2.2.2).

In iCORAL we consider only net carbonate production; i.e., there is no explicit computation of gross production or dissolution. In the current study, the impact of coral reef carbonate production on the global carbon cycle is not considered, as its effect is likely to be small on centennial timescales.

A previous study comparing model results with existing data of coral reef carbonate production and location has shown comparatively good agreement (Bouttes et al., 2024). The global mean carbonate production simulated in the model is 0.81 Pg $CaCO_3$ yr^{-1}, which lies in the range of data estimates from 0.65 to 0.83 Pg $CaCO_3$ yr^{-1} (Vecsei, 2004). The model simulates a global coral reef area of 390×10^3 km^2, also in the range of observations, although these have large uncertainty, ranging from 150×10^3 km^2 to

1500×10^3 km^2 (Smith, 1978; Crossland et al., 1991; Copper, 1994; Spalding et al., 2001; Vecsei, 2004; Li et al., 2020). The model correctly simulates the presence of coral reef in most locations where they are observed but also in a few places where there are no observations to date (Bouttes et al., 2024).

2.2 Simulations

We have run an ensemble of 31 simulations under historical and future greenhouse gas concentration scenarios, testing different hypotheses with regard to climate model climate sensitivity, coral reef thermal bleaching adaptation and socioeconomic scenarios. All simulations were run from 1850 (starting from an equilibrated 1850 run) to 2300 with prescribed atmospheric CO_2, CH_4 and N_2O concentrations for the historical period and the different Shared Socioeconomic Pathways (SSPs; Meinshausen et al., 2020). These concentrations are publicly available and were downloaded from the Earth System Grid Federation (ESG, https://esgf-node.llnl.gov/search/input4mips/, last access: 22 June 2023). Changes in land use and concentrations of atmospheric aerosols are not considered in the iLOVECLIM simulations.

2.2.1 Equilibrium climate sensitivity (ECS)

The simulated ocean warming in response to atmospheric CO_2 emissions and the resulting impact of this on coral reefs are strongly dependent on the equilibrium climate sensitivity (ECS) of a given model. The ECS is the equilibrium global mean near-surface temperature change in response to a doubling of atmospheric CO_2 concentration compared to the preindustrial period (i.e., from ∼ 280 to 560 ppm) and is often computed by regressing the top-of-atmosphere radiative flux against the global average surface air temperature change (Gregory et al., 2004). The ECS varies greatly among climate models, from around 1.5 up to 5.6 °C in CMIP6 (Forster et al., 2020; Meehl et al., 2020). Based on several lines of evidence, the very likely range of IPCC AR6 for the ECS is 2 to 5 °C and the likely range 2.5 to 4.0 °C (Forster et al., 2021).

We test the impact of different climate sensitivities by spanning a range of possible equilibrium climate sensitivities within the iLOVECLIM model. The standard iLOVECLIM ECS is at the lower range, at ∼ 2 °C (Fig. 1). We can, however, vary ECS in the model by modifying the α parameter used in the longwave radiation (LWR) code following Timm and Timmerman (2007):

$$\mathrm{LWR} = \alpha a\left(\lambda, \varphi, p, t_{\mathrm{season}}\right) \log\left[\frac{\mathrm{CO_2}\,(t)}{\mathrm{CO_2}\,(t0)}\right],$$

where $CO_2(t0) = 356$ ppm is the reference CO_2 concentration. The transfer coefficient a is a function of longitude, latitude, height and season (Chou and Neelin, 1996).

In this study, the ECS is computed as the difference between the mean of the last 100 years of equilibrium simulation with $2\times CO_2$ and the preindustrial simulation for each α value. The α parameter is varied between 1 (standard simulation) and 3. While the standard ECS with $\alpha = 1$ is 2 °C, it increases to 5.4 °C with $\alpha = 3$. With $\alpha = 1.5$, the ECS is 2.9 °C, thus falling within the AR6 likely range (Fig. 1). We have chosen this value to run additional simulations with different SSP scenarios and idealized experiments to analyze the response of coral reefs.

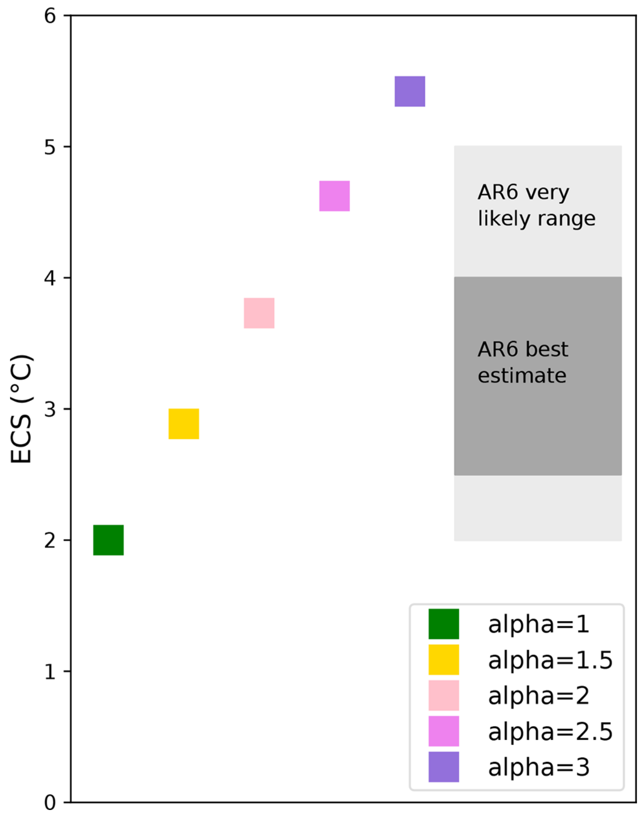

Figure 1. Equilibrium climate sensitivity (ECS, °C) in iLOVECLIM computed after 2000 years of simulation compared to the estimated range from IPCC AR6 (Forster et al., 2021).

2.2.2 Coral thermal adaptation to bleaching

The potential adaptation of coral reefs to thermal conditions that can cause bleaching is poorly constrained (Cooley et al., 2022). We thus consider two contrasting cases of coral adaptation to bleaching: one with no adaptation and one with continuous adaptation.

In the coral reef module, the bleaching of corals is simulated when the cumulative temperature anomaly passes a threshold following the degree heating week (DHW) approach adopted in NOAA's Coral Reef Watch (CRW) program for the purpose of bleaching prediction (https://www.coralreefwatch.noaa.gov/product/5km/methodology.php#dhw, last access: 28 October 2024). In each grid cell, the temperature anomaly is computed with respect to a reference, which is the maximum of the climatological monthly mean temperature over 30 years, i.e., the temperature of the hottest month in the climatological monthly means for each grid element (maximum of the climatological monthly mean temperature, MMM). It is thus assumed that accumulated thermal stress is the primary driver of mass bleaching events. This is of course a simplification, and the method has substantial associated uncertainty – see Klein et al. (2024) for an extensive discussion of the strengths and weaknesses of this so-called "excess heat" threshold model (as well as those of alternatives, such as population dynamic, species distribution or ecology–evolutionary models). It should be noticed that different taxa have different responses to thermal stress and local temperature variability also plays a role (McClanahan et al., 2020). The predictive power of the method can be improved if, e.g., region-specific threshold values are adopted (DeCarlo, 2020). Here we decided to closely follow the original Coral Reef Watch methodology as it is most suitable for the level of complexity of the climatic forcings that iLOVECLIM can provide. We furthermore use the original global threshold values as iCORAL does not carry any information about the reef ecosystem structure and does therefore not allow for any regional differentiation. Other stress factors besides excess heat that may lead to bleaching, such as anomalously low temperatures, anomalous nutrient concentrations and salinities, are already considered in the habitability criteria.

In the simulations, we evaluate the impact of possible coral adaptation on the thermal threshold for bleaching by changing the reference period used to calculate the MMM. Assuming non-adaptation, this reference is computed from the first 30 years of the simulations (hence from 1850 to 1879) and kept fixed. On the contrary, if we assume adaptation to changing temperature (referred to as "thermal adaptation to bleaching" in the following), this temperature reference evolves with time and is computed from the 30-year running mean.

2.2.3 Greenhouse gas scenarios

We run each simulation starting from 1850 under the historical scenario followed by different SSPs (Fig. 2). Depending on the simulation, we consider SSP1-1.9, SSP1-2.6, SSP2-4.5, SSP3-7.0, SSP5-3.4-OS or SSP5-8.5 (O'Neill et al., 2016; Meinshausen et al., 2020). For each ECS, with- and without thermal adaptation to bleaching, we run simulations with the low-emission scenario SSP1-2.6 and the high-emission scenario SSP5-8.5 to bound the projected response of coral reef habitability and carbonate production (Table 1). In the case of the mid-range ECS of 2.9 °C (for $\alpha = 1.5$) we have additionally run simulations with all SSPs to evaluate more precisely the impact of the different scenarios (Table 1).

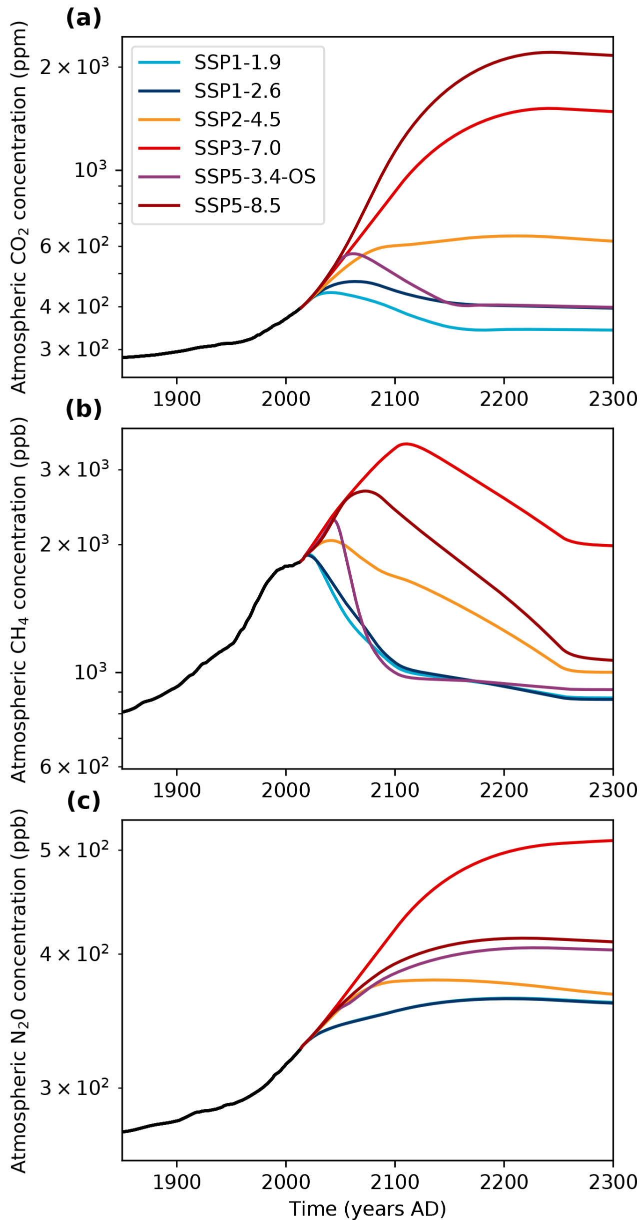

Figure 2. Evolution of atmospheric CO_2, CH_4 and N_2O for the different SSP scenarios (data from Meinshausen et al., 2020).

2.2.4 Relative roles of warming and acidification

Finally, we have also run idealized SSP5-8.5 simulations with an ECS of 2.9 °C ($\alpha = 1.5$) where coral reef habitability and carbonate production are considered to be (i) independent of temperature (including bleaching), (ii) independent of Ω_{ar}, and (iii) independent of both temperature (including bleaching) and Ω_{ar} (Table 1). The temperature and Ω_{ar} that coral reefs experience in these idealized simulations are set to those reached at the end of the first simulated year (i.e., 1850), removing the impact of warming and acidification on carbonate production. These simulations al-

Table 1. Overview of the climate scenario and model climate sensitivity combinations used for the simulation experiments. All simulations marked by a plus sign (+) were carried out in two variants: one with coral thermal adaptation to bleaching (moving 30-year reference climatology) and one without (reference climatology fixed to first 30 years of the simulation). For the SSP5-8.5 scenario, three additional simulations were carried out to allow for a simple factor impact analysis: "ΩT " for which the T and Ω_{ar} distributions seen by the corals are kept fixed at the values prevailing at the end of the first simulation year; "T" for which only the temperature distribution is kept fixed, but the Ω_{ar} distribution evolves as calculated by the carbon cycle model; "Ω" for which the Ω_{ar} is kept fixed, but T follows the evolution calculated by the climate model. For these three, bleaching adaptation was disabled.

α	1.0	1.5	2.0	2.5	3.0
Scenario					
SSP1-1.9		+			
SSP1-2.6	+	+	+	+	+
SSP2-4.5		+			
SSP3-7.0		+			
SSP5-3.4-OS		+			
SSP5-8.5	+	+	+	+	+
		ΩT,T, Ω			

low analysis of the individual impacts of warming, acidification and bleaching on coral reef habitability and carbonate production, allowing assessment of the relative importance of these stressors and potential nonlinearities when there is compound stressor exposure.

3 Results

3.1 Temperature and pH

The main environmental variables controlling coral reef carbonate production in the model are temperature and Ω_{ar}. While temperature is available from CMIP6 models, Ω_{ar} is not a standard output, so we compare results for pH, which is closely related to Ω_{ar}. The sea surface temperatures in iLOVECLIM are similar to the CMIP6 temperatures in terms of time evolution (Fig. 3a and b). However, the amplitude of the warming is smaller in iLOVECLIM compared to CMIP6. Even with high ECS, the warming in iLOVECLIM is in the low range of CMIP6 projections. Hence the resulting coral reef production simulated by the model might be conservative in the sense that its decline might be underestimated. The evolution of the pH is very similar in iLOVECLIM and CMIP6. It does not depend on the ECS as it is mainly driven by the atmospheric CO_2 concentration.

3.2 Projected coral reef distribution and carbonate production

During the historical period, the coral production decreases very slowly, from 0.81 Pg $CaCO_3$ yr^{-1} in 1850 to 0.74 Pg $CaCO_3$ yr^{-1} in 1970 (Fig. 4). At the end of the 20th century, the production starts decreasing more strongly in all simulations, but the evolution diverges depending on scenarios and the possibility of adaptation.

3.2.1 Without thermal adaptation to bleaching

In the iLOVECLIM simulations without bleaching adaptation that have an ECS of 2.9 °C, coral carbonate production rapidly declines under all SSPs in the early 21st century (Fig. 4, left panel). The rate of this decline is however lower with high-mitigation scenarios such as SSP1-1.9 and SSP1-2.6. By 2100, coral reef carbonate production either ceases entirely (SSP 2-4.5, SSP3-7.0, SSP5-8.5) or stabilizes at 25 % or less of the preindustrial value (SSP1-1.9, SSP1-2.6). With the overshoot scenario (SSP5-3.4-OS) carbonate production stops and then slightly recovers, albeit at a very low level.

3.2.2 With thermal adaptation for bleaching

Bleaching adaptation strongly modifies the results of our projections of coral reef carbonate production over the next three centuries (Fig. 4, right panel). Across all scenarios, the rate of carbonate production decline is reduced, with some carbonate production still occurring in all scenarios in 2100 (contrary to the simulations without adaptation).

Under the high-emission scenarios SSP3-7.0 and SSP5-8.5, coral reef carbonate production still eventually ceases (or becomes negligibly small in the case of SSP3-7.0), albeit $\sim$ 140 years later than when no bleaching adaptation is assumed ($\sim$ 2060 without adaptation vs. $\sim$ 2200 with adaptation). By 2100, carbonate production is still considerably diminished with SSP5-8.5, with the location of net-accreting coral reefs reduced in all oceans (Fig. 5d) compared to the preindustrial period (Fig. 5a). Under SSP2-4.5 (medium emissions) reef carbonate production decreases and stabilizes at around half the preindustrial value and by 2100 most coral reef locations are still net accreting (Fig. 5c).

Carbonate production initially decreases and then partially recovers under the high-mitigation scenarios (SSP1-1.9 and SSP1-2.6) as well as under the overshoot scenario (SSP5-3.4-OS), with most coral reef locations returning to net accreting in 2100 (Fig. 5b). With the overshoot scenario, regions where coral reefs were not accreting by $\sim$ 2050 can become net accreting again in the following years as coral production recovers (Fig. 6).

At the end of the 21st century under the high-mitigation scenario SSP1-2.6, global reef carbonate production is 10 % of the preindustrial value if there is no bleaching adaptation

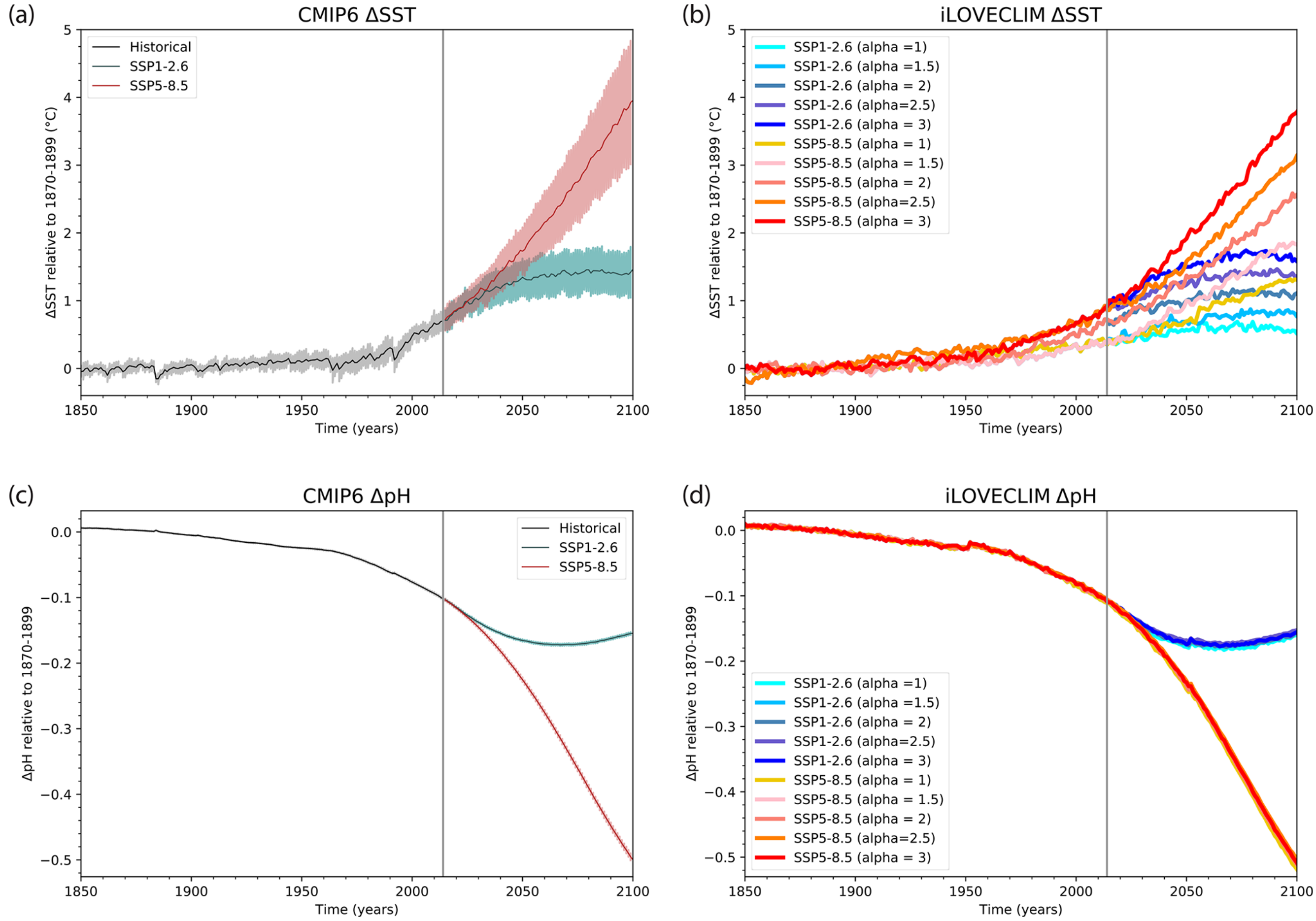

Figure 3. Evolution of global sea surface temperature and pH for CMIP6 models compared to the iLOVECLIM model for SSP1-2.6 and SSP8-5.8. The variables are anomalies with respect to the mean value for 1870-1899. The CMIP6 data are from Kwiatkowski et al. (2020).

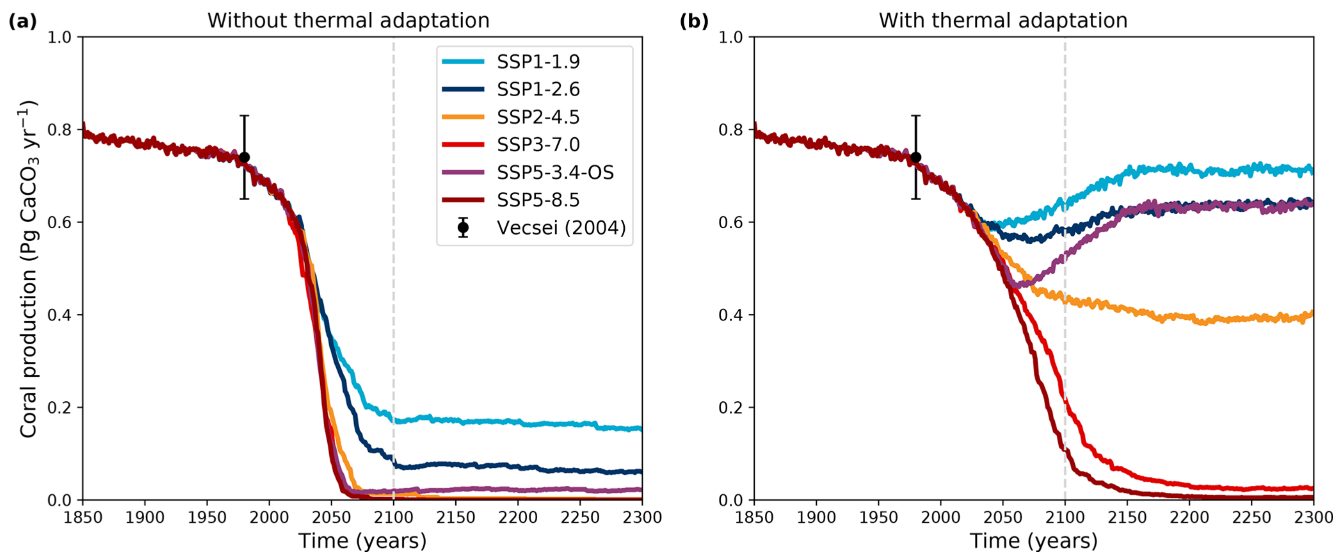

Figure 4. Dynamics of the global coral reef $CaCO_3$ production (Pg $CaCO_3$ yr^{-1}) over the historical simulation and for different SSP scenarios **(a)** without and **(b)** with thermal adaptation to bleaching. The iLOVECLIM version used for these simulations has an ECS of 2.9 °C ($\alpha = 1.5$, Fig. 1). The circle with whiskers indicates estimates of the modern data of $CaCO_3$ production (Vecsei, 2004).

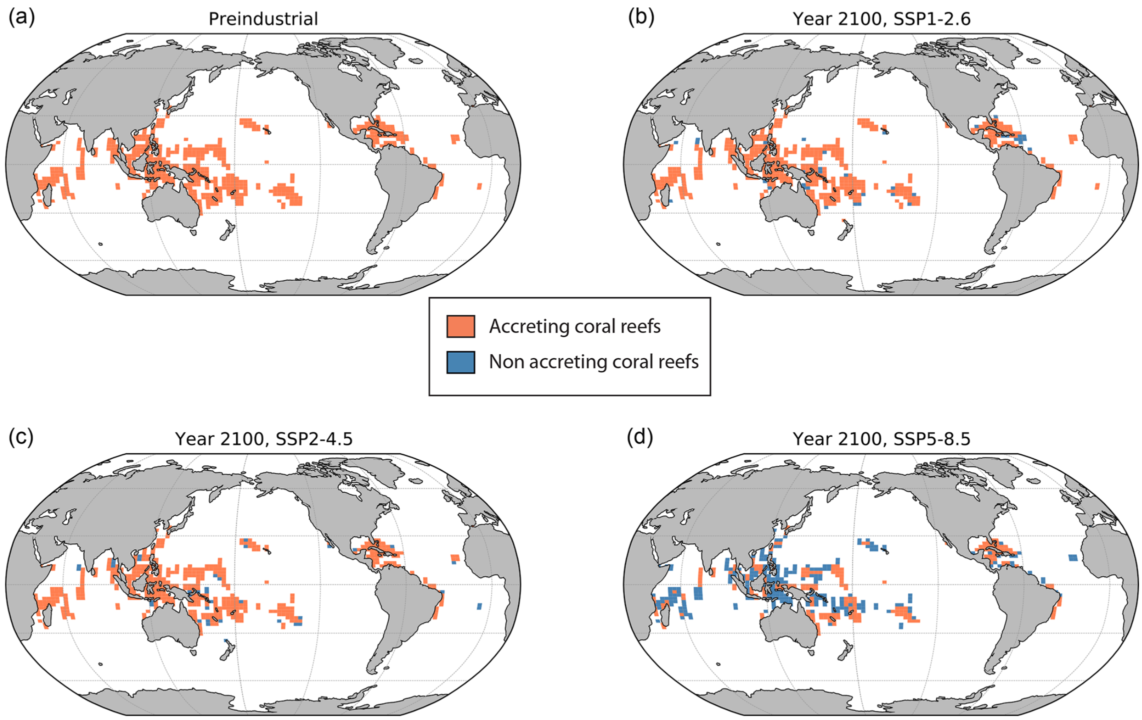

Figure 5. Simulated distributions of net-accreting coral reefs under **(a)** preindustrial conditions and in 2100 (mean of 2095-2105) under **(b)** SSP1-2.6, **(c)** SSP2-4.5 and **(d)** SSP5-8.5. An ECS of 2.9 °C ($\alpha = 1.5$) was adopted for all simulations, and thermal adaptation to bleaching was activated.

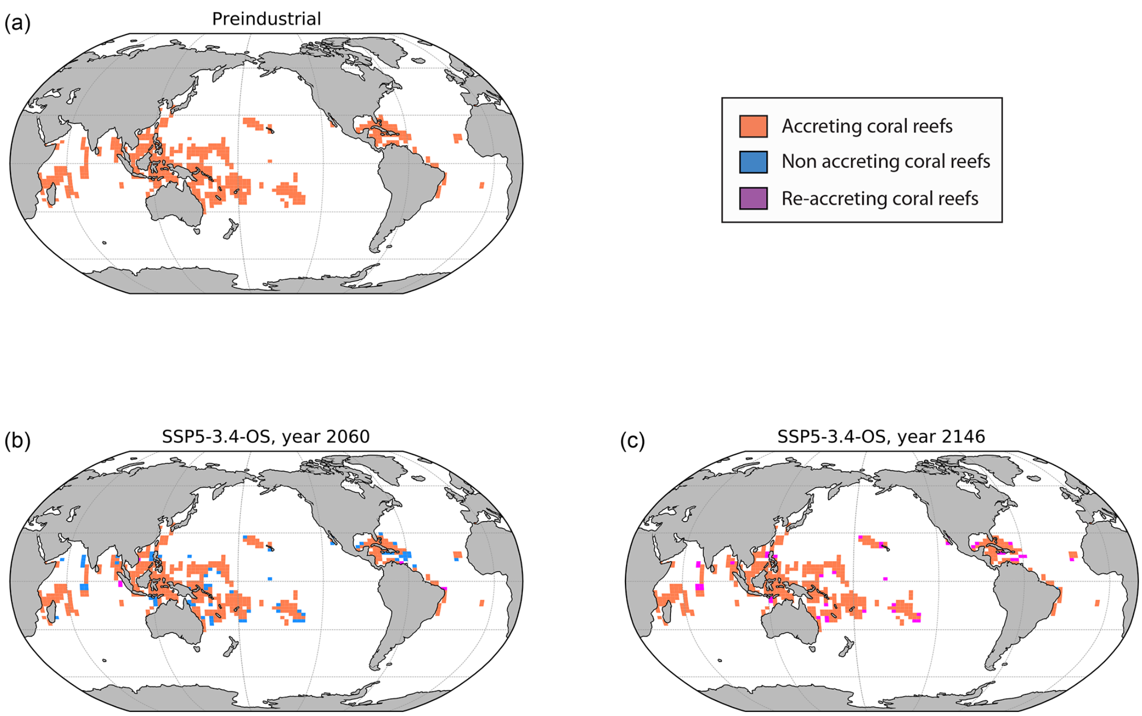

Figure 6. Simulated distributions of net-accreting coral reefs under **(a)** preindustrial conditions and in SSP3.4-OS at **(b)** the year 2060 (compared to preindustrial) and **(c)** the year 2146 (compared to year 2060). An ECS of 2.9 °C ($\alpha = 1.5$) was used for this simulation, and thermal adaptation to bleaching was activated.

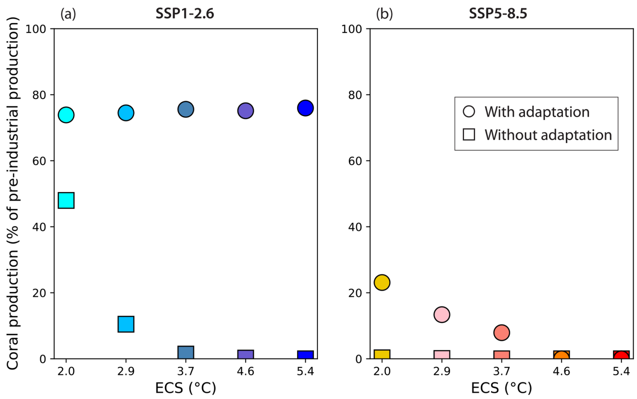

Figure 7. Percentage of preindustrial global coral reef carbonate production simulated in the year 2100 for SSP1-2.6 and SSP5-8.5 across ECS values (percentage values are 2090–2110 means relative to 1850–1870 mean carbonate production).

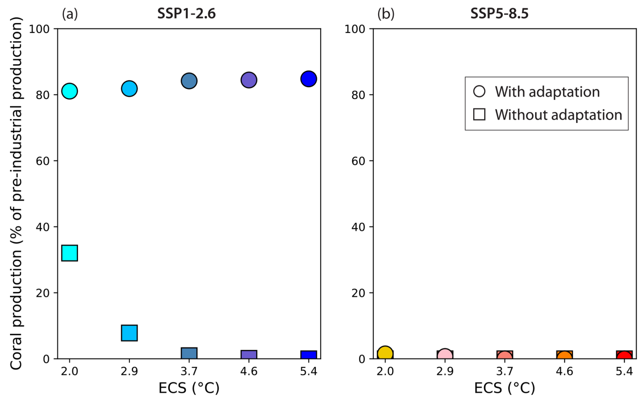

Figure 8. Percentage of preindustrial global coral reef carbonate production simulated in the year 2300 for **(a)** SSP1-2.6 and **(b)** SSP5-8.5 across ECS values (percentage values are 2280–2300 means relative to 1850–1870 mean carbonate production).

compared to 70 % with adaptation. With SSP5-8.5, carbonate production ceases entirely without adaptation but is reduced to 10 % of the preindustrial with adaptation (Fig. 7).

3.3 Impact of equilibrium climate sensitivity

Across the range of ECS values, the large difference in the projected carbonate production between high-mitigation (SSP1-2.6) and high-emission (SSP5-8.5) simulations is maintained when adaptation is considered (circles in Fig. 7). With SSP1-2.6, the temperature and saturation state changes are much smaller than with SSP5-8.5 (Fig. 3). Accordingly, the global carbonate production decrease is smaller with SSP1-2.6 than with SSP5-8.5, as both increased temperature and decreased saturation state tend to lower production. In addition, when we let the reference temperature climatology for bleaching evolve with time, coral reefs have time to adapt to such temperature changes and will be less prone to bleaching. By 2100, this leads to a relatively small decrease in carbonate production of less than 30 % (production is maintained at levels above 70 % of the preindustrial value) with SSP1-2.6. On the contrary, with SSP5-8.5 the temperature and Ω_{ar} changes are much larger, and the temperature change is too fast for corals to adapt sufficiently to avoid bleaching. This results in a greater than 75 % decrease in carbonate production by 2100 (<25 % of preindustrial carbonate production).

If no adaptation is considered (squares in Fig. 7), with SSP1-2.6 carbonate production in the simulations decreases with increasing ECS, as there is greater ocean warming. By 2100, it has decreased to levels between 0 % to 50 % of the preindustrial production. With SSP5-8.5, ocean warming is so strong that carbonate production ceases before the end of the 21st century for all ECS values.

3.4 Long-term (after 2100) changes in carbonate production

After 2100, with SSP1-2.6 carbonate production partially recovers when thermal adaptation is considered so that it is higher in 2300 (at ∼ 80 %) compared to 2100 (at ∼ 70 %) but still lower than the preindustrial level (circles in Fig. 8, left panel, compared to Fig. 7, left panel). Without adaptation, the carbonate production remains low or ceases (squares in Fig. 8, left panel). With SSP5-8.5, the coral reef carbonate production drops to zero, when it has not already done so before, in all simulations even when thermal adaptation to bleaching is considered (Fig. 8, right panel).

3.5 Relative influence of warming and acidification

To evaluate the relative role of saturation state and temperature (including bleaching) we have run idealized simulations by removing separately (or in combination) their limiting effects on carbonate production (Fig. 9). Having neither temperature nor Ω_{ar} limitation (blue line, "other drivers") results in a persistent coral reef carbonate production, showing that future changes in other variables such as nutrients or light do not significantly influence coral production. The reduction in Ω_{ar} suppresses simulated carbonate production. When only Ω_{ar} limitation is accounted for in coral production (effect of acidification, no temperature limitation considered, green line), carbonate production initially responds similarly to the standard simulations with all limiting variables (red line). However, around the year 2030 the temperature starts to play a larger limiting role (effect of warming, no Ω_{ar} limitation, orange line). Hence both temperature (including bleaching) and Ω_{ar} play a crucial role in governing coral production, with Ω_{ar} being the main limiting factor in the early part of the simulation, while temperature becomes the main limiting variable later. The effects of warming and acidification com-

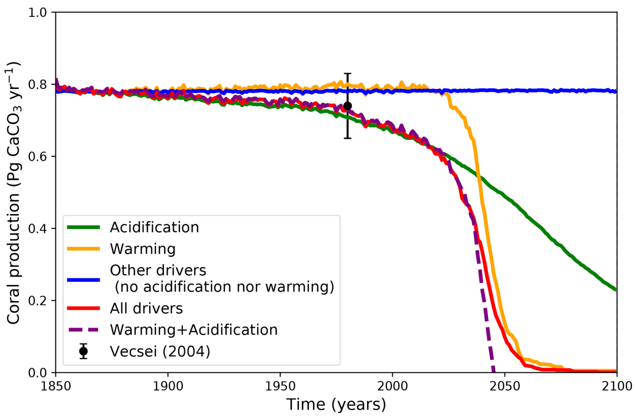

Figure 9. The projected impact of acidification, warming and other drivers on global coral reef carbonate production ($Pg\,CaCO_3\,yr^{-1}$) for ECS = 2.9 °C ($\alpha = 1.5$) for the historical plus SSP5-8.5 scenarios. Simulations are without thermal adaptation to bleaching. The dashed purple line is the linear combination of the warming and acidification effects.

bine linearly during the first part of the evolution until around the year 2040, corresponding to slightly less than 50 % of the production decline (purple line compared to red line). The response of the production then becomes nonlinear, with a saturation of the production decline which tends to mainly follow the effect of warming.

4 Discussion

4.1 Comparison with past studies

While most previous studies focused on specific regions or only accounted for the individual impact of warming or acidification, Cornwall et al. (2021, 2023) quantified future global changes in coral reef calcification in response to changes in both temperature and Ω_{ar}. They used a different method, based on statistical functions derived from observations. For the future, they used model outputs from simulations forced by RCP scenarios. Although the new SSP scenarios are different, RCP2.6 and SSP1-2.6, as well as RCP8.5 and SSP5-8.5, are comparable (Meinshausen et al., 2020). By construction, the SSP and corresponding RCP scenarios have the same radiative forcing in 2100 (e.g., $8.5\,W\,m^{-2}$ for RCP8.5 and SSP5-8.5). However, as discussed in Kwiatkowski et al. (2020) the greenhouse gas emissions, hence concentrations, differ due to different mixes of energy sources. For example, the CO_2 concentration is higher under SSP5-8.5 compared to RCP8.5, which results in greater ocean acidification in SSP5-8.5 compared to RCP8.5.

By 2100, Cornwall et al. (2021) projected a decline in global mean net carbonate production of 77 % for RCP2.6 with negative global net production (erosion) and no reefs able to accrete at rates equivalent to projected sea level rise for RCP8.5. With our coupled climate–coral model net erosion is not currently permissible; however we do project complete cessation of net accretion by 2100 for SSP5-8.5 (in the absence of thermal adaptation). For SSP1-2.6 the projected impact on carbonate production strongly depends on the model ECS. It varies from a 50 % reduction with a very low ECS to complete cessation with high ECS. Cornwall et al. (2023) additionally considered possible coral adaptation to warming (symbiont evolution and symbiont shuffling) based on ecological modeling (Logan et al., 2021). They showed that the main factor driving carbonate production was the emission scenario, with adaptation changing the severity of the impacts. Adaption only had a significant effect in the low-emission scenario (RCP2.6) in this study. We also note a larger impact of thermal adaptation with the low-emission scenario. However, with low ECS thermal adaptation also modifies the resulting carbonate production. In our simulations, thermal adaptation is not considered through ecological parameterizations such as in Logan et al. (2021), which would be too complex relative to the rest of the model. We consider thermal adaptation through changes in the reference temperature for the bleaching scheme. With adaptation, the time window used to compute the temperature reference (the maximum of the climatological monthly mean temperature over 30 years) evolves, while it is kept constant (at the beginning of the simulation) otherwise. This thermal adaptation strongly modifies the results in our simulations, especially for low-emission scenarios like SSP1-2.6, where the carbonate production decline is substantially reduced compared to the simulations without thermal adaptation and maintained above 70 % of preindustrial levels for SSP1-2.6 across all ECS values. Hence, we obtain similar values, especially without thermal adaptation, but we show that accounting for different climate sensitivities, which would correspond to uncertainties among climate models, also results in large differences. In addition, thermal adaptation strongly modifies the resulting carbonate production, in particular with high-emission scenarios but also with low-emission scenarios when combined with low ECS.

4.2 Caveats and missing processes

Because we have embedded a coral reef carbonate production module within a climate model, the results depend on the climate simulated by the model. In iLOVECLIM, the temperature change tends to be at the lower end of the range covered by CMIP6 simulations. Hence, simulated carbonate production reductions might be underestimated. iLOVECLIM has a relatively coarse ocean resolution of 3° by 3° on the horizontal grid. While we have been able to take into account the spatial heterogeneity of the seafloor topography by adopting a subgrid parametrization, this is not possible for other variables such as temperature, as they depend on local circulation dynamics. Hence the model cannot account for small-scale features such as local temperature and Ω_{ar} changes. A consequence of this is that while large-scale changes can be evaluated with the model, local changes dependent on small-scale dynamics cannot be simulated. Such limitations could be partially addressed by the use of a higher-resolution model in which the same coral module could be implemented. In addition, higher-resolution models also have a higher temporal resolution, resulting in better tropical variability, which would further improve the modeled coral reef response.

The coral reef carbonate production module strongly relies on current knowledge of the coral reef response to environmental variables. Large uncertainties remain, and better understanding of coral reef responses will help improve the coral module in the future. For example, the relationship between Ω_{ar} and the rate of calcification is complex (Chan and Connolly, 2013; Jokiel, 2016; Eyre et al., 2018). As corals can control their internal pH value and seem to be more sensitive to pH (Comeau et al., 2018), carbonate production might need to depend on pH instead of saturation state. Further research is required to refine the model parameterizations. In addition, we have shown that the possibility of adaptation to thermal stress results in a wide range of responses. More constraints on the potential for adaptation (e.g., Logan et al., 2021) will help to reduce the range of future coral reef carbonate production projections.

4.3 Perspectives

A current limitation in the coral reef module is the use of a common function to represent the response of all coral reefs to environmental conditions. Coral species respond differently to changes in temperature and Ω_{ar} (Klepac et al., 2023), and species composition differs across reefs. In addition, the different components of coral reefs (coral, algae, crustose coralline algae, sediment) also substantially differ across reefs, and each has different sensitivities to temperature and saturation state changes (Kroeker et al., 2010; Eyre et al., 2018; Leung et al., 2022). A future improvement could thus be to consider several coral functional types, allowing, for example, for reefs dominated by branched vs. massive corals, similarly to what is done in land vegetation models with plant functional types.

In the coral reef module, we compute net carbonate production, which represents the net difference between production and destruction (erosion and dissolution) in an implicit manner. However, we do not explicitly simulate the impact of bioeroders, such as sponges, or crown-of-thorns starfish. As they play an important role in counteracting carbonate production (Schönberg et al., 2017), accounting for them could improve the model, but this would require a complex ecological model.

Finally, we do not consider other anthropogenic impacts on corals, such as pollution or overfishing, which can further degrade living conditions for coral reefs, or local or regional management, which can offset some of that stress (Wolff et al., 2018).

5 Conclusions

Using a global coupled coral–climate model, we have shown diverse carbonate production changes from coral reefs in future projections. The large range of carbonate production changes stems from uncertainties in scenarios (socioeconomic uncertainties), climate sensitivities (climate model uncertainties) and thermal adaptation (coral reef biology uncertainties). With the high-emission SSP5-8.5 scenario, global coral reef carbonate production drops dramatically or ceases, regardless of the equilibrium climate sensitivity (ECS) and potential thermal adaptation to bleaching. Only with a low ECS and thermal adaptation to bleaching can coral reef carbonate production be kept stable under SSP5-8.5, albeit at a fraction of the preindustrial value (less than 25 % of the preindustrial value with ECS = 2 °C in 2100). On the contrary, with the low-emission SSP1-2.6 scenario, the potential range of future coral reef carbonate production is much larger and can reach 76 % of the preindustrial value in 2100 (with ECS = 5.4 °C and thermal adaptation). Carbonate production depends strongly on the possibility of thermal adaptation. For SSP1-2.6 without thermal adaptation, global carbonate production drops to between 0 % and 48 % of preindustrial values in 2100 and between 0 % and 32 % of preindustrial values in 2300. With thermal adaptation, the production decreases are much more moderate: the carbonate production drops to between 73 % and 76 % of preindustrial values by 2100, recovering to between 81 % and 85 % by 2300. With the SSP5-3.4 overshoot scenario, the conditions can become habitable for coral reefs to become net carbonate accretors again in some regions, but this assumes that larvae are available to repopulate these regions.

Code availability. The code of the iCORAL module is available on Zenodo (https://doi.org/10.5281/zenodo.7985881; Bouttes et al., 2023).

Data availability. The data that support the findings of this study are openly available on Zenodo at https://doi.org/10.5281/zenodo.12958336 (Bouttes, 2024).

Author contributions. NB: conceptualization; funding acquisition; investigation; methodology; writing – original draft preparation; writing – review and editing. LK: conceptualization; methodology; writing – review and editing. EB: investigation. MB: investigation. VB: conceptualization; methodology; writing – review and editing. GM: conceptualization; methodology; writing – review and editing.

Competing interests. The contact author has declared that none of the authors has any competing interests.

Disclaimer. Publisher's note: Copernicus Publications remains neutral with regard to jurisdictional claims made in the text, published maps, institutional affiliations, or any other geographical representation in this paper. While Copernicus Publications makes every effort to include appropriate place names, the final responsibility lies with the authors.

Acknowledgements. We thank Didier Roche for his support with the iLOVECLIM model. We thank the reviewers and editor for their comments which helped improve this paper.

Financial support. Financial support for this work was provided by the Belgian Fund for Scientific Research – F.R.S.-FNRS (project SERENATA, grant no. CDR J.0123.19). Guy Munhoven is a research associate with the Belgian Fund for Scientific Research – F.R.S.-FNRS. Victor Brovkin acknowledges funding by the European Research Council (ERC) as part of the Q-Arctic project (grant agreement no. 951288). Lester Kwiatkowski acknowledges funding by the European Research Council (ERC) as part of the TipESM project (grant agreement no. 101137673) and the ENS Chanel research chair. The authors acknowledge the ANR – FRANCE (French National Research Agency) for its financial support of the TICMY project no. 273305.

Review statement. This paper was edited by Tyler Cyronak and reviewed by Christopher Cornwall and one anonymous referee.

References

Albright, R., Caldeira, L., Hosfelt, J., Kwiatkowski, L., Maclaren, J. K., Mason, B. M., Nebuchina, Y., Ninokawa, A., Pongratz, J., Ricke, K. L., Rivlin, T., Schneider, K., Sesboüé, M., Shamberger, K., Silverman, J., Wolfe, K., Zhu, K., and Caldeira, K.: Reversal of ocean acidification enhances net coral reef calcification, Nature, 531, 362–365, https://doi.org/10.1038/nature17155, 2016.

Albright, R., Takeshita, Y., Koweek, D., Ninokawa, A., Wolfe, K., Rivlin, T., Nebuchina, Y., Young, J., and Caldeira, K.: Carbon dioxide addition to coral reef waters suppresses net community calcification, Nature, 555, 516–519, https://doi.org/10.1038/nature25968, 2018.

Bouttes, N.: Coral reef carbonate production simulations with iLOVECLIM-iCORAL, Zenodo [data set], https://doi.org/10.5281/zenodo.12958336, 2024.

Bouttes, N., Roche, D. M., Mariotti, V., and Bopp, L.: Including an ocean carbon cycle model into iLOVECLIM (v1.0), Geosci. Model Dev., 8, 1563–1576, https://doi.org/10.5194/gmd-8-1563-2015, 2015.

Bouttes, N., Kwiatkowski, L., Berger, M., Brovkin, V., and Muhnoven, G.: iCORAL code (1.0), Zenodo [code], https://doi.org/10.5281/zenodo.7985881, 2023.

Bouttes, N., Kwiatkowski, L., Berger, M., Brovkin, V., and Munhoven, G.: Implementing the iCORAL (version 1.0) coral reef $CaCO_3$ production module in the iLOVECLIM climate model, Geosci. Model Dev., 17, 6513–6528, https://doi.org/10.5194/gmd-17-6513-2024, 2024.

Brown, B. E.: Coral bleaching: causes and consequences, Coral Reefs, 16, S129–S138, https://doi.org/10.1007/s003380050249, 1997.

Buddemeier, R. W., Jokiel, P. L., Zimmerman, K. M., Lane, D. R., Carey, J. M., Bohling, G. C., and Martinich, J. A.: A modeling tool to evaluate regional coral reef responses to changes in climate and ocean chemistry, Limnol. Oceanogr.-Meth., 6, 395–411, https://doi.org/10.4319/lom.2008.6.395, 2008.

Buddemeier, R. W., Lane, D. R., and Martinich, J. A.: Modeling regional coral reef responses to global warming and changes in ocean chemistry: Caribbean case study, 109, 375–397, Climatic Change, https://doi.org/10.1007/s10584-011-0022-z, 2011.

Chan, N. C. S. and Connolly, S. R.: Sensitivity of coral calcification to ocean acidification: a meta-analysis, Glob. Change Biol., 19, 282–290, https://doi.org/10.1111/gcb.12011, 2013.

Chou, C. and Neelin, J. D.: Linearization of a long-wave radiation scheme for intermediate tropical atmospheric model, J. Geophys. Res., 101, 15129–15145, https://doi.org/10.1029/96JD01015, 1996.

Comeau, S., Cornwall, C. E., DeCarlo, T. M., Krieger, E., and McCulloch, M. T.: Similar controls on calcification under ocean acidification across unrelated coral reef taxa, Glob. Change Biol., 24, 4857–4868, https://doi.org/10.1111/gcb.14379, 2018.

Cooley, S., Schoeman, D., Bopp, L., Boyd, P., Donner, S., Ghebrehiwet, D. Y., Ito, S.-I., Kiessling, W., Martinetto, P., Ojea, E., Racault, M.-F., Rost, B., and Skern-Mauritzen, M.: Ocean and Coastal Ecosystems and their Services. In: Climate Change 2022: Impacts, Adaptation, and Vulnerability. Contribution of Working Group II to the Sixth Assessment Report of the Intergovernmental Panel on Climate Change, edited by: Pörtner, H.-O., Roberts, D. C., Tignor, M., Poloczanska, E. S., Mintenbeck, K., Alegría, A., Craig, M., Langsdorf, S., Löschke, S., Möller, V., Okem, A., and Rama, B., Cambridge University Press, Cambridge, UK and New York, NY, USA, 379–550, https://doi.org/10.1017/9781009325844.005, 2022.

Copper, P.: Ancient reef ecosystem expansion and collapse, Coral Reefs, 13, 3–11, https://doi.org/10.1007/BF00426428, 1994.

Cornwall, C. E., Comeau, S., Kornder, N. A., and Lowe, R. J.: Global declines in coral reef calcium carbonate production under ocean acidification and warming, 118, e2015265118, https://doi.org/10.1073/pnas.2015265118, 2021.

Cornwall, C. E., Comeau, S., Donner, S. D., Perry, C., Dunne, J., van Hooidonk, R., Ryan, J. S., and Logan, C. A.: Coral adaptive capacity insufficient to halt global transition of coral reefs into net erosion under climate change, Glob. Chang Biol., 29, 3010–3018, https://doi.org/10.1111/gcb.16647, 2023.

Couce, E., Ridgwell, A., and Hendy, E. J.: Future habitat suitability for coral reef ecosystems under global warming and ocean acidification, Glob. Change Biol., 19, 3592–3606, https://doi.org/10.1111/gcb.12335, 2013.

Crossland, C. J., Hatcher, B. G., and Smith, S. V.: Role of coral reefs in global ocean production, Coral Reefs, 10, 55–64, https://doi.org/10.1007/BF00571824, 1991.

DeCarlo, T. M.: Treating coral bleaching as weather: a framework to validate and optimize prediction skill, PeerJ, 8, e9449, https://doi.org/10.7717/peerj.9449, 2020.

DeCarlo, T. M., Harrison, H. B., Gajdzik, L., Alaguarda, D., Rodolfo-Metalpa, R., D'Olivo, J., Liu, G., Patalwala, D., and McCulloch, M. T.: Acclimatization of massive reef-building corals to consecutive heatwaves, Proc. R. Soc. B, 286, 20190235, https://doi.org/10.1098/rspb.2019.0235, 2019.

Donner, S.D., Skirving, W.J., Little, C.M., Oppenheimer, M., and Hoegh-Guldberg, O.: Global assessment of coral bleaching and required rates of adaptation under climate change, Glob. Chang Biol., 11, 2251–2265, https://doi.org/10.1111/j.1365-2486.2005.01073.x, 2005.

Dove, S. G., Kline, D. I., Pantos, O., Angly, F. E., Tyson, G. W., and Hoegh-Guldberg, O.: Future reef decalcification under a business-as-usual CO_2 emission scenario, P. Natl. Acad. Sci. USA, 110, 15342–15347, https://doi.org/10.1073/pnas.1302701110, 2013.

Evenhuis, C., Lenton, A., Cantin, N. E., and Lough, J. M.: Modelling coral calcification accounting for the impacts of coral bleaching and ocean acidification, Biogeosciences, 12, 2607–2630, https://doi.org/10.5194/bg-12-2607-2015, 2015.

Eyre, B. D., Cyronak, T., Drupp, P., De Carlo, E. H., Sachs, J. P., and Andersson, A. J.: Coral reefs will transition to net dissolving before end of century, Science, 359, 908–911, https://doi.org/10.1126/science.aao1118, 2018.

Forster, P., Storelvmo, T., Armour, K., Collins, W., Dufresne, J.-L., Frame, D., Lunt, D. J., Mauritsen, T., Palmer, M. D., Watanabe, M., Wild, M., and Zhang, H.: The Earth's Energy Budget, Climate Feedbacks, and Climate Sensitivity. In Climate Change 2021: The Physical Science Basis. Contribution of Working Group I to the Sixth Assessment Report of the Intergovernmental Panel on Climate Change, edited by: Masson-Delmotte, V., Zhai, P., Pirani, A., Connors, S. L., Péan, C., Berger, S., Caud, N., Chen, Y., Goldfarb, L., Gomis, M. I., Huang, M., Leitzell, K., Lonnoy, E., Matthews, J. B. R., Maycock, T. K., Waterfield, T., Yelekçi, O., Yu, R., and Zhou, B., Cambridge University Press, Cambridge, United Kingdom and New York, NY, USA, 923–1054, https://doi.org/10.1017/9781009157896.009, 2021.

Forster, P. M., Maycock, A. C., McKenna, C. M., and Smith, C. J.: Latest climate models confirm need for urgent mitigation, Nat. Clim. Change, 10, 7–10, https://doi.org/10.1038/s41558-019-0660-0, 2020.

Frieler, K., Meinshausen, M., Golly, A., Mengel, M., Lebek, K., Donner, S. D., and Hoegh-Guldberg, O.: Limiting global warming to 2 °C is unlikely to save most coral reefs, Nat. Clim. Change, 3, 165–170, https://doi.org/10.1038/nclimate1674, 2012.

Frölicher, T. L., Fischer, E. M., and Gruber, N.: Marine heatwaves under global warming, Nature, 560, 360–364, https://doi.org/10.1038/s41586-018-0383-9, 2018.

Goosse, H., Brovkin, V., Fichefet, T., Haarsma, R., Huybrechts, P., Jongma, J., Mouchet, A., Selten, F., Barriat, P.-Y., Campin, J.-M., Deleersnijder, E., Driesschaert, E., Goelzer, H., Janssens, I., Loutre, M.-F., Morales Maqueda, M. A., Opsteegh, T., Mathieu, P.-P., Munhoven, G., Pettersson, E. J., Renssen, H., Roche, D. M., Schaeffer, M., Tartinville, B., Timmermann, A., and Weber, S. L.: Description of the Earth system model of intermediate complexity LOVECLIM version 1.2, Geosci. Model Dev., 3, 603–633, https://doi.org/10.5194/gmd-3-603-2010, 2010.

Gregory, J. M., Ingram, W. J., Palmer, M. A., Jones, G. S., Stott, P. A., Thorpe, R. B., Lowe, J. A., Johns, T. C., and Williams, K. D.: A new method for diagnosing radiative forcing and climate sensitivity, Geophys. Res. Lett., 31, L03205, https://doi.org/10.1029/2003GL018747, 2004.

Hoegh-Guldberg, O.: Climate change, coral bleaching and the future of the world's coral reefs, Mar. Freshwater Res., 50, 839–866, https://doi.org/10.1071/MF99078, 1999.

Hoegh-Guldberg, O., Poloczanska, E. S., Skirving, W., and Dove, S.: Coral Reef Ecosystems under Climate Change and Ocean Acidification, Front. Mar. Sci., 4, 158, https://doi.org/10.3389/fmars.2017.00158, 2017.

Jokiel, P. L.: Predicting the impact of ocean acidification on coral reefs: evaluating the assumptions involved, ICES J. Mar. Sci., 73, 550–557, https://doi.org/10.1093/icesjms/fsv091, 2016.

Klein, S. G., Roch, C. and Duarte, C. M.: Systematic review of the uncertainty of coral reef futures under climate change, Nat. Commun., 15, 2224, https://doi.org/10.1038/s41467-024-46255-2, 2024

Klepac, C. N., Eaton, K. R., Petrik, C. G., Arick, L. N., Hall, E. R., and Muller, E. M.: Symbiont composition and coral genotype determines massive coral species performance under end-of-century climate scenarios, Front. Mar. Sci., 10, 1026426, https://doi.org/10.3389/fmars.2023.1026426, 2023.

Kleypas, J. A.: A diagnostic model for predicting global coral reef distribution, in: Recent Advances in Marine Science and Technology '94", edited by: Bellwood, O., Choat, H., and Saxena, N., PACON International and James Cook University, 211–220, https://nla.gov.au/nla.cat-vn2172300, 1995.

Kleypas, J. A.: Modeled estimates of global reef habitat and carbonate production since the Last Glacial Maximum, Paleoceanography, 12, 533–545, https://doi.org/10.1029/97PA01134, 1997.

Kleypas, J. A., Buddemeier, R. W., Archer, D., Gattuso, J.-P., Langdon, C., and Opdyke, B. N.: Geochemical consequences of increased atmospheric carbon dioxide on coral reefs, Science, 284, 118–120, https://doi.org/10.1126/science.284.5411.118, 1999.

Kroeker, K. J., Kordas, R. L., Crim, R. N., and Singh, G. G.: Meta-analysis reveals negative yet variable effects of ocean acidification on marine organisms, Ecol. Lett., 13, 1419–1434, https://doi.org/10.1111/j.1461-0248.2010.01518.x, 2010.

Kwiatkowski, L., Torres, O., Bopp, L., Aumont, O., Chamberlain, M., Christian, J. R., Dunne, J. P., Gehlen, M., Ilyina, T., John, J. G., Lenton, A., Li, H., Lovenduski, N. S., Orr, J. C., Palmieri, J., Santana-Falcón, Y., Schwinger, J., Séférian, R., Stock, C. A., Tagliabue, A., Takano, Y., Tjiputra, J., Toyama, K., Tsujino, H., Watanabe, M., Yamamoto, A., Yool, A., and Ziehn, T.: Twenty-first century ocean warming, acidification, deoxygenation, and upper-ocean nutrient and primary production decline from CMIP6 model projections, Biogeosciences, 17, 3439–3470, https://doi.org/10.5194/bg-17-3439-2020, 2020.

Langdon, C., and Atkinson, M. J.: Effect of elevated pCO2 on photosynthesis and calcification of corals and interactions with seasonal change in temperature/irradiance and nutrient enrichment, J. Geophys. Res., 110, C09S07, https://doi.org/10.1029/2004JC002576, 2005.

Leung, J. Y. S., Zhang, S., and Connell, S. D.: Is Ocean Acidification Really a Threat to Marine Calcifiers? A Systematic Review and Meta-Analysis of 980+ Studies Spanning Two Decades, Small, 18, 2107407, https://doi.org/10.1002/smll.202107407, 2022.

Li, J., Knapp, D. E., Fabina, N. S., Kennedy, E. V., Larsen, K., Lyons, M. B., Murray, N. J., Phinn, S. R., Roelfsema, C. M., and Asner, G. P.: A global coral reef probability map generated using convolutional neural networks, Coral Reefs, 39, 1805–1815, https://doi.org/10.1007/s00338-020-02005-6, 2020.

Logan, C. A., Dunne, J. P., Ryan, J. S., Baskett, M. L., and Donner, S.: Quantifying global potential for coral evolutionary response to climate change, Nat. Clim. Chang., 11, 537–542, https://doi.org/10.1038/s41558-021-01037-2, 2021.

McClanahan, T. R., Darling, E. S., Maina, J. M., Muthiga, N. A., D'agata, S., Leblond, J., Arthur, R., Jupiter, S. D., Wilson, S. K., Mangubhai, S., Ussi, A. M., Guillaume, M. M. M., Humphries, A. T., Patankar, V., Shedrawi, G., Pagu, J., and Grimsditch, G.: Highly variable taxa-specific coral bleaching responses to thermal stresses, Mar. Ecol. Prog. Ser., 648, 135–151, https://doi.org/10.3354/meps13402, 2020.

Meehl, G. A., Senior, C. A., Eyring, V., Flato, G., Lamarque, J. F., Stouffer, R. J., Taylor, K. E., and Schlund, M.: Context for interpreting equilibrium climate sensitivity and transient climate response from the CMIP6 Earth system models, Sci Adv., 6, eaba1981, https://doi.org/10.1126/sciadv.aba1981, 2020.

Meinshausen, M., Nicholls, Z. R. J., Lewis, J., Gidden, M. J., Vogel, E., Freund, M., Beyerle, U., Gessner, C., Nauels, A., Bauer, N., Canadell, J. G., Daniel, J. S., John, A., Krummel, P. B., Luderer, G., Meinshausen, N., Montzka, S. A., Rayner, P. J., Reimann, S., Smith, S. J., van den Berg, M., Velders, G. J. M., Vollmer, M. K., and Wang, R. H. J.: The shared socioeconomic pathway (SSP) greenhouse gas concentrations and their extensions to 2500, Geosci. Model Dev., 13, 3571–3605, https://doi.org/10.5194/gmd-13-3571-2020, 2020.

O'Neill, B. C., Tebaldi, C., van Vuuren, D. P., Eyring, V., Friedlingstein, P., Hurtt, G., Knutti, R., Kriegler, E., Lamarque, J.-F., Lowe, J., Meehl, G. A., Moss, R., Riahi, K., and Sanderson, B. M.: The Scenario Model Intercomparison Project (ScenarioMIP) for CMIP6, Geosci. Model Dev., 9, 3461–3482, https://doi.org/10.5194/gmd-9-3461-2016, 2016.

Pandolfi, J. M., Connolly, S. R., Marshall, D. J., and Cohen, A. L.: Projecting Coral Reef Futures Under Global Warming and Ocean Acidification, Science, 333, 418-422, https://doi.org/10.1126/science.1204794, 2011.

Schönberg, C. H. L., Fang, J. K. H., Carreiro-Silva, M., Tribollet, A., and Wisshak, M.: Bioerosion: the other ocean acidification problem, ICES J. Mar. Sci., 74, 895–925, https://doi.org/10.1093/icesjms/fsw254, 2017.

Silverman, J., Lazar, B., Cao, L., Caldeira, K., and Erez, J.: Coral reefs may start dissolving when atmospheric CO_2 doubles, Geophys. Res. Lett., 36, L05606, https://doi.org/10.1029/2008GL036282, 2009.

Smith, S.: Coral-reef area and the contributions of reefs to processes and resources of the world's oceans, Nature, 273, 225–226, https://doi.org/10.1038/273225a0, 1978.

Spalding, M., Spalding, M. D., Ravilious, C., and Green, E. P.: World atlas of coral reefs, University of California Press, 2001.

Sully, S., Burkepile, D.E., Donovan, M.K., Hodgson, G., and van Woesik, R.: A global analysis of coral bleaching over the past two decades, Nat Commun. 10, 1264, https://doi.org/10.1038/s41467-019-09238-2, 2019.

Sully, S., Hodgson, G., and van Woesik, R.: Present and future bright and dark spots for coral reefs through climate change, Glob. Change Biol., 10, 1264, https://doi.org/10.1111/gcb.16083, 2022.

Timm, O. and Timmermann, A.: Simulation of the Last 21 000 Years Using Accelerated Transient Boundary Conditions, J. Climate, 20, 4377–4401, https://doi.org/10.1175/JCLI4237.1, 2007.

van Hooidonk, R., Maynard, J. A., Manzello, D., and Planes, S.: Opposite latitudinal gradients in projected ocean acidification and bleaching impacts on coral reefs, Glob. Change Biol., 20, 103–112, https://doi.org/10.1111/gcb.12394, 2014.

Vecsei, A.: A new estimate of global reefal carbonate production including the fore-reefs, Global Planet. Change, 43, 1–18, https://doi.org/10.1016/j.gloplacha.2003.12.002, 2004.

Wolff, N. H., Mumby, P. J., Devlin, M., and Anthony K. R. N.: Vulnerability of the Great Barrier Reef to climate change and local pressures, Glob. Change Biol., 24, 1978–1991, https://doi.org/10.1111/gcb.14043, 2018.